IMPROVED B-SPLINE SKINNING APPROACH FOR DESIGN OF HAWT BLADE MOLD SURFACES

S. F. Hosseini **B. Moetakef-Imani***

Department of Mechanical Engineering
Ferdowsi University of Mashhad (FUM)
Mashhad, Iran

ABSTRACT

The intricate 3D design of wind turbine blades has caused unwanted problems for blade designers and blade mold manufacturers. For example the cord length variation and twisting of airfoils, change of the airfoil type and the blade pre-bend can introduce major geometric complications. A novel method is suggested to improve 3D modeling of the blade mold surfaces as well as the required parting lines during the design process of the wind turbine blade. In the proposed algorithm, the blade leading edge surface is trimmed by parting lines calculated based on the blade silhouette while keeping G^1 continuity of resulting surfaces. The Minimum Variation Surface (MVS) and strain energy fairing criteria approve that blade mold surfaces obtained by the developed method have better fairness compared to the surface created by the well-established design method. All programs are written in MATLAB and the final surfaces are converted into the standard IGES file format which is importable into any commercial CAD/CAM system..

Keywords: Wind turbine blade, Mold surface, Parting lines, Skinning.

1. INTRODUCTION

B-Spline and NURBS (Non-Uniform Rational B-Spline) representations along with wealth of developed algorithms have become a very strong tool in designing 3D model of complicated and sculptured surfaces [1]. Advanced feature of surface skinning based on B-splines is an important design method for various types of wind turbine blade[2, 3].

The design of wind turbine blades usually starts with the selection of airfoil types developed for wind turbine applications[4, 5]. When the required geometrical parameters of the selected airfoil, i.e. chord length, twist angle and position of the airfoil center relative to the rotor blade center, are determined the x- and y-coordinates of the airfoil will be available. Figure 1 shows the standard airfoil points of an S823 National Renewable Energy Laboratory (NREL) airfoil [6]. Section Curves are then approximated from these standard data points [7].

In the computer aided design of the Horizontal Axis Wind Turbine (HAWT), the blade surface is constructed by implementing skinning method to the scaled, twisted and translated airfoils along the blade length. The common practice in commercial CAD systems indicates that the skinning process will introduce some geometric issues[8]. For example, undesired curvature variations and the broken continuity can be introduced during skinning of the blade surface. Some improvements on the surface can be obtained by time consuming trial and error methods, however it is not recommended for nowadays applications. Some researchers have enhanced the B-spline skinning algorithms by selecting a compatible parameter vector for all section curves which seems plausible for the design of HAWT blades.

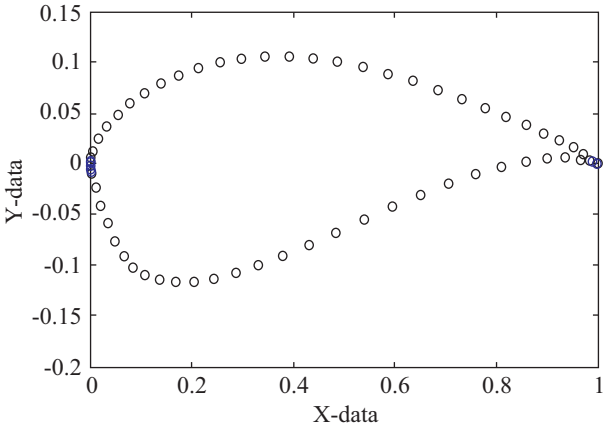

Fig. 1 Airfoil points of an S823 NREL airfoil [6].

Among the applied research works on the above mentioned subjects, Shamsuddin *et al.* [9] developed a NURBS

* Corresponding author (imani@um.ac.ir)

DOI : 10.1017/jmech.2016.79

Fig. 2 Parting Lines in the leading and trailing edges of a typical wind turbine blade.

skinning approach for ship hull design. They have addressed the problem of generating a ship hull from non-regular cross section curves. Presenting a new compatibility process, they have built a fair surface for ship hull manufactured by one mold. Hampsey [10] have developed a B-spline skinning method for aerodynamic and structural optimizations of wind turbine blades. Although the skinning compatibility is addressed, the constructed surface is limited to the aerodynamic part of the blade. It should be noted that the root section of the blade requires further consideration. Perez *et al*. [11] implemented a B-spline surface representation of wind turbine blades passing through airfoil section points. Although they have constructed section curves which accurately approximate the airfoil points in the leading edge region, the automatic creation of parting lines and mold surfaces with desired continuity is still an unsolved problem. In addition, manufacturing aspects of the blade mold are required to take into consideration in the early design stages of wind turbine blades. Other related researches may be found in refs [12-14].

Current design and manufacturing processes of a HAWT blade typically involve several manual steps. Producing a 3D model of a wind turbine blade during designing process which can be directly used in a mold manufacturing process will strongly reduce the time required for new products. In practice, two mold cavities will be created after finishing the design of blade's 3D model. Due to twisting and in some cases pre-bending of the 3D model of the blade, the parting lines would be complicated 3D curves. In fact, parting lines of a HAWT blade are on one side the trailing edge of the blade and on the other side the silhouette of the leading edge surface, see Fig. 2 for details. In order to impose desired continuity on the two mold surfaces, the current research proposes to design each part of the blade's mold separately. In this way, the desired continuity for the leading edge parting line and the trailing edge would be achieved. In addition, the curvature variations of two parts of the blade's mold are dealt with separately and would be within the desired values.

Henceforth the paper is organized as follows. In Section 2, the curve approximation method with specified end derivatives is introduced. Section 3 briefly presents the NURBS skinning process and common compatibility issues reported in practice. The curve approximation applied to the HAWT's airfoils is addressed in the next section. In Section 5, a B-spline surface for each part of the blade's mold is constructed. In addition, the Minimum Variation Surface (MVS) fairing criterion computed for the developed method, i.e. designing two separate skinned surfaces, is compared to that of a single surface skinning approach. This section also addresses the design considerations proposed for the blade root region. The last section concludes the paper and discusses the results.

2. CURVE APPROXIMATION WITH END DERIVATIVES SPECIFIED

A B-spline curve of degree p is defined as follows:

$$\mathrm{C(u)}=\sum_{i=0}^{\mathrm{n}} n_{i,p}(u)P_i \tag{1}$$

where P_i are the control points and $N_{i,p}$ are the B-spline basis functions defined over the knot vector by

$$U=\left\{\underbrace{0,\ldots,0}_{p+1},u_{p+1},\ldots,u_{m-p-1},\underbrace{1,\ldots,1}_{p+1}\right\}$$

Suppose that a set of input airfoil points Q_r $r = 0, \ldots, m$ and derivatives at start and end points as $D_s^{(1)},\ldots,D_s^{(k)}$ and $D_e^{(1)},\ldots,D_e^{(l)}$ respectively are given where $k, l < p$. Using a chord length parameterization and knot vector generation according to [1], a two-step approximation procedure reported in [15] was used for approximation:

2.1 Compute the End Control Points Using the Following Equations:

$$\begin{aligned}
&P_0=Q_0\\
&P_i=\frac{1}{N_{i,p}^{(i)}(t_0)}\left[D_s^{(i)}\sum_{h=0}^{i-1}n_{h,p}^{(i)}(t_0)P_h\right],\quad i=0,\ldots,k\\
&P_n=Q_m\\
&P_{n-j}=\frac{1}{N_{n-j,p}^{(j)}(t_m)}\left[D_e^{(j)}\sum_{h=0}^{j-1}N_{n-h,p}^{(j)}(t_m)P_{n-h}\right],\quad j=0,\ldots,l
\end{aligned} \tag{2}$$

2.2 Compute the Rest of Control Points with Least Square Minimization:

$$\sum \left| Q_r - c(t_r) \right|^2 = \min \tag{3}$$

The control points $P_0, \ldots, P_n$ are the unknowns of the problem and derivation on how to compute them is given in [1].

3. SKINNING

The extension of the B-spline theory to a tensor product of two B-spline curves results in a B-spline surface definition:

$$S(u,v) = \sum_{i=0}^{n} \sum_{j=0}^{m} N_{i,p}(u) N_{j,q}(v) P_{i,j} \tag{4}$$

where p and q are surface degrees in u and v directions, respectively, and $P_{i,j}{}_{\substack{i=0,\ldots,n \\ j=0,\ldots,m}}$ are a net of control points defined by $P_{i,j} = (x_{i,j}, y_{i,j}, z_{i,j})$. Also $N_{i,p}(u)$, $i = 0, \ldots, n$ and $N_{j,q}(v)$, $j = 0, \ldots, m$ are B-spline basis functions in u and v directions which are defined on the following knot vectors, respectively:

$$U = \left\{ \underbrace{0,\ldots,0}_{p+1}, u_{p+1}, \ldots, u_{r-p-1}, \underbrace{1,\ldots,1}_{p+1} \right\}$$

$$V = \left\{ \underbrace{0,\ldots,0}_{q+1}, v_{q+1}, \ldots, v_{s-q-1}, \underbrace{1,\ldots,1}_{q+1} \right\}$$

In the skinning process, a B-spline surface approximates section curves in the v direction. Each section curve is denoted as bellow:

$$C_k(u), \quad k = 0, \ldots, 1$$

A very important requirement for the quality of skinning is the compatibility of section curves which means that the degree of section curves must be equal and they have to be defined over the same knot vector. The degree is an input in the curve approximation process, and should be set equal for all section curves. Knot vectors depend on parameters assigned to the data points. Thus, distribution of data points can affect parameters and its associated knot vector.

There are two types of compatibility methods in the literature, exact methods and approximate methods. In exact methods, a common knot vector is considered to be the union of all section curves' knot vectors [1]. A knot insertion algorithm is then applied to each section curve to make them compatible. Although this method is exact, the computational cost is huge, therefore approximate methods are introduced which can strongly reduce the computational cost [16-18]. In a wind turbine blade, cross section curves are airfoils which are apparently of the same shape, so, as an approximate solution, we consider the common knot vector to be the average of the unique knot vectors of all sections. The next step is to approximate the curves again with the common knot vector. The least square error shows the accuracy of the new approximations. The details of this procedure are presented in the next section.

4. AIRFOIL CURVE APPROXIMATION

The wind turbine blade designers propose the airfoil type, chord length, twist angle and the fitting tolerance value and quality at each radial section. It should be pointed out that the blade root section starts with a circular curve, followed by successive airfoil curves which are approximated by B-spline curves. In addition, 2D airfoils should be converted into a 3D airfoil for better aerodynamic performance, see [11, 12]. The process of 2D to 3D conversion is shown in Fig. 3.

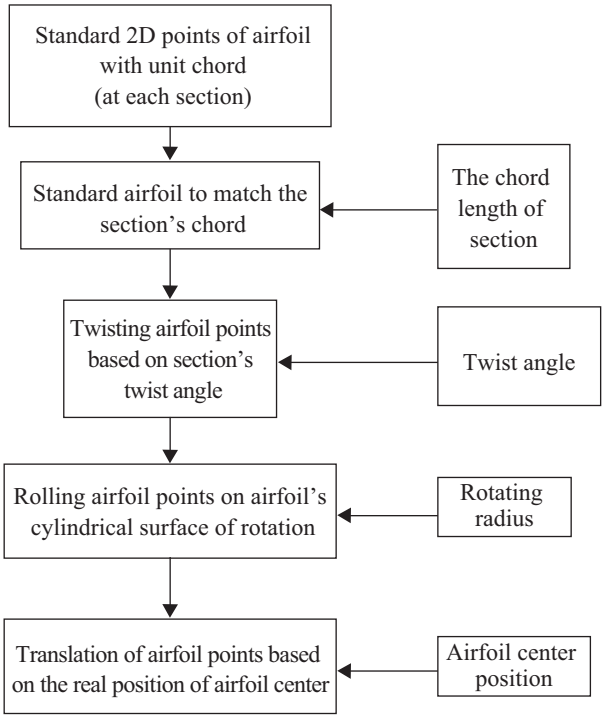

Fig. 3 The process of 2D to 3D conversion of airfoil points.

The steps described in Fig. 3 can be formulated by the following equations [11]:

$$\begin{aligned} Q_i' &= (x', y') = (c_i x'', c_i y'') \\ R &= \sqrt{x'^2 + y'^2} \\ \theta &= \tan -1\left(\frac{y'}{x'}\right) \\ \alpha_1 &= R\cos(\theta + Tw_i) \\ Q_i &= (r_i \sin(\alpha_i), R\sin(\theta + Tw_i), r_i \cos(\alpha_i)) \end{aligned} \tag{5}$$

where x'' and y'' are the input 2D airfoil points and c_i, r_i and Tw_i are the chord length, radius and twist angle of

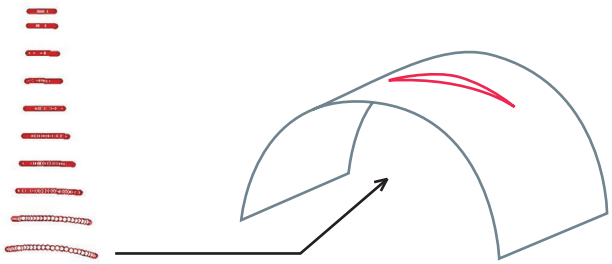

Fig. 4 3D airfoils lie on their rotation cylinder.

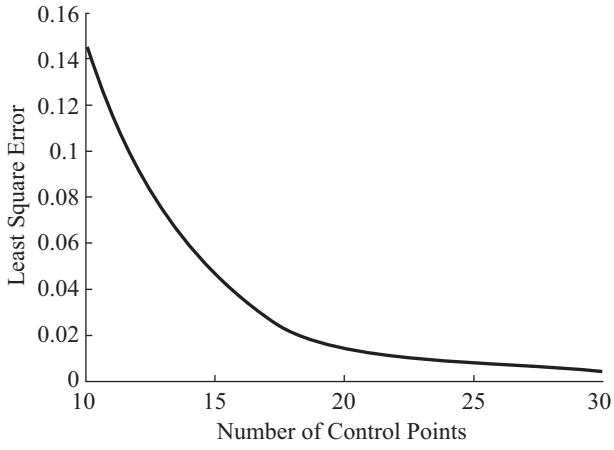

Fig. 5 The variation of the least square error with respect to the number of approximation control points.

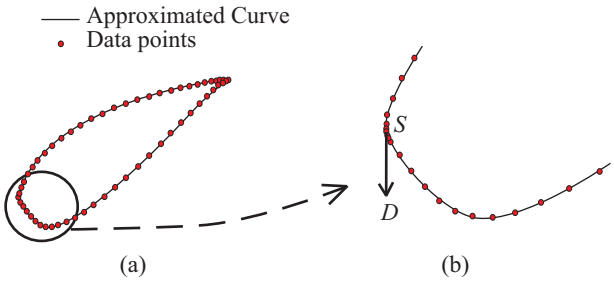

Fig. 6 Curve approximation on airfoil points: (a) A typical curve approximation with 15 control points and (b) Desired division point where the tangent vector is vertical.

the i'th section, respectively. Figure 4 shows the 3D data points (Q_i) created from Eq. (5).

In curve approximation, the least square error highly depends on the number of control points as depicted in Fig. 5 for an S823 NREL airfoil [6].

A schematic representation of a S823 airfoil approximation is also shown in Fig. 6.

Point S, where the tangent vector is vertical, lies on the silhouette curve required for designing upper and lower blade mold surfaces. In fact, taking manufacturing issues in to consideration at the design stage would be most beneficial for mold manufacturer. Thus, point *S* could be considered as the division point which divides the airfoil into upper and lower set of points which are approximated separately. Due to the extreme importance of the blade leading edge geometry on the aerodynamic performance of the wind turbine, G^1 continuity should be imposed at the leading edge region while C^0 continuity is sufficient at the trailing edge region.

In this research a constraint based approximation is implemented which is required for better aerodynamic performance. The intensity of G^1continuity can highly improve the accuracy of approximation in the leading edge region, as shown in Fig. 7. On the other hand, due to the local modification property of B-spline curves, the other areas of upper and lower curves are not affected. A Sequential Quadratic Programming (SQP) optimization procedure is proposed for computing the desired value of the tangent vector, which is denoted by D in Fig. 6. It should be noted that the least square error is our objective function of the constraint based approximation. The optimized values depend on the number of approximation control points as depicted in Fig. 7 for an S823 NREL airfoil.

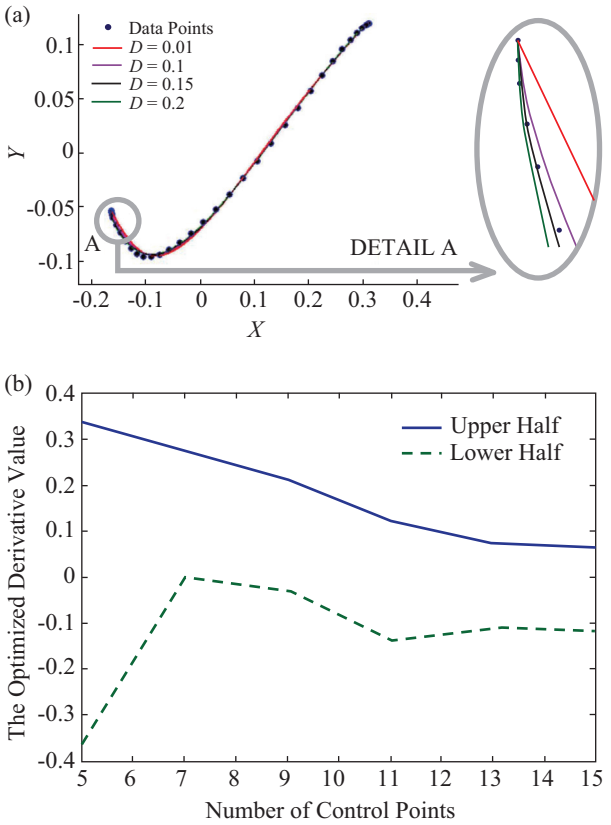

Fig. 7 Optimizingthe intensity of tangency (a) Curve approximation with different end derivative values and (b) The optimized value versus the number of control points for the upper and lower surfaces.

Approximating each airfoil section with two constrained curves has two main advantages. Firstly, the mold surfaces are created directly. In practice, the process of creating mold surfaces from a single twisted surface in the commercial CAD software is complicated

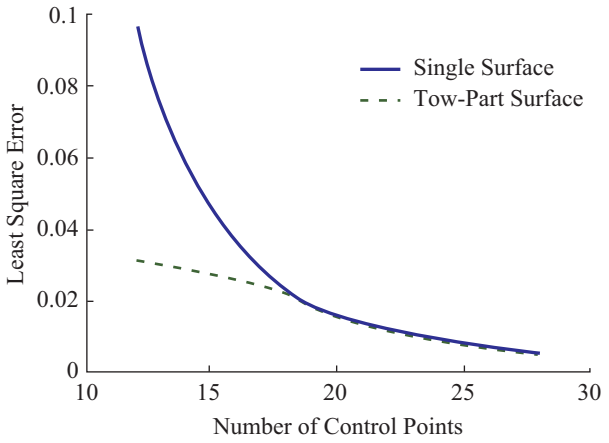

Fig. 8 The variation of the approximation least square error versus the number of control points for single and two-part blade surfaces.

and can be the source of molding problems. The second advantage is that for a constant number of control points, the least square approximation error is decreased. This advantage is demonstrated in Fig. 8.

According to this figure, it is obvious that the least square error of a two-part surface is lower than a single surface. Also in low number of control points, it is highly recommended to use the two-part method. It should be noted that the proposed method is faster than the traditional single surface method which is very significant if higher number of approximation control points (n) are needed. At each section curve, the traditional method needs inverting an n by n matrix for the least square process (Eq. 3), while the proposed method suggests inverting two n/2 by n/2 matrix that strongly reduces the computational time and efforts.

5. MOLD SURFACE DESIGN

After approximating a series of B-spline curves for the desired sections, a B-spline surface can be approximated. The control points of each section are treated as intermediate control points and a curve approximation on each column of control points will lead to a B-spline surface. Based on the proposed algorithm, for each part of the blade surface, a B-spline surface is constructed. A visual comparison between the mold surfaces constructed from the proposed (improved) and traditional (original) approaches can be made using SolidWorks curvature analysis as depicted in Fig. 9.

Figure 9 indicates that the curvature variations in the mold surfaces constructed from the proposed approach is less compared to those of traditional approach. In addition to the advantages which are mentioned in Section 4 for the section curve design, the Minimum Variation Surface (MVS) and strain energy fairing criteria computed for the upper and lower blade surfaces improve compared to the usual single surface approach. The MVS and strain energy values of a surface can be obtained using the following integrals [19]:

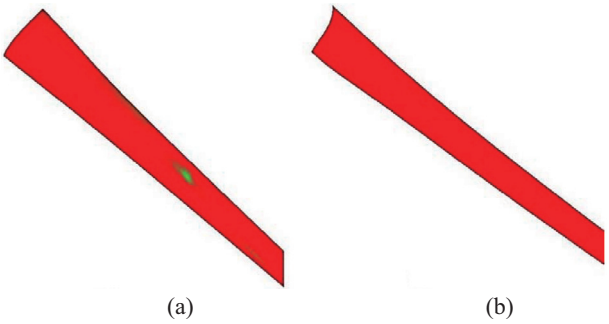

Fig. 9 SolidWorks curvature analysis for (a) blade's upper part constructed from the traditional approach, (b) blade's upper part constructed from the proposed approach.

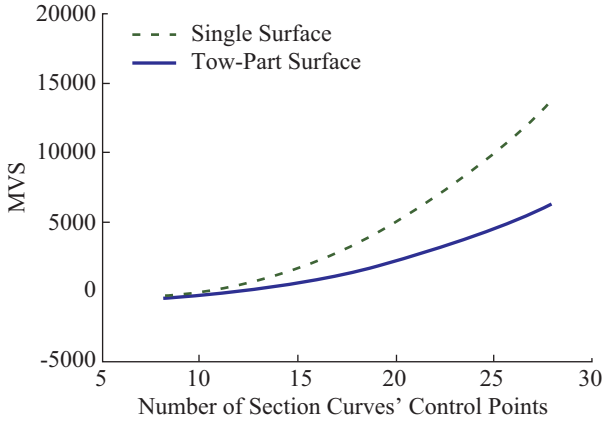

Fig. 10 The variation of MVS value with respect to the number of control points in u-direction for single and two-part surfaces.

$$MVS = \int \left(\left[\frac{\partial \kappa_1}{\partial e_1} \right]^2 + \left[\frac{\partial \kappa_2}{\partial e_2} \right]^2 \right) dA$$
$$\text{Strain Energy} = \int (\kappa_1^2 + \kappa_2^2)\, dA \qquad (6)$$

where κ_1 and κ_2 are principal curvatures and e_1 and e_2 are the principal directions. From quantitative point of view, lower MVS value is interpreted as lower curvature variations. The difference between the total MVS and strain energy values of a single vs. two-part blade surface construction are demonstrated in Figs. 10 and 11 respectively.

The two-part blade construction has a lower total MVS value versus a single-part blade as depicted in Fig. 10. The lower MVS values, which mean lower curvature variations, improve aerodynamic performance of the blades [20, 21]. The final surfaces are converted into an IGES standard file format to help us import them directly into commercial CAD and FEM software. An example of the final molds is shown in Fig. 12.

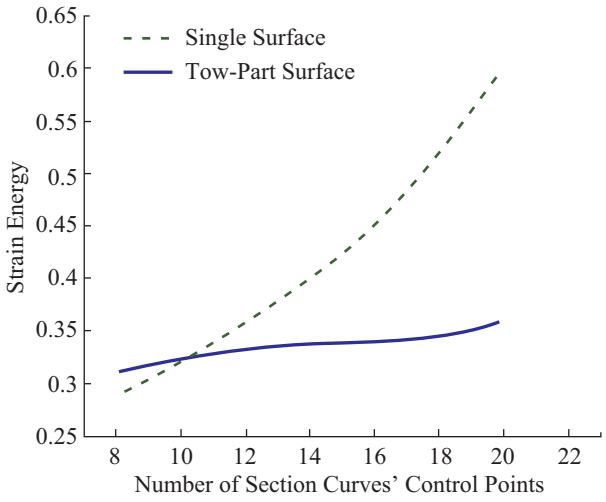

Fig. 11 The variation of strain energy value with respect to the number of control points in u-direction for single and two-part surfaces.

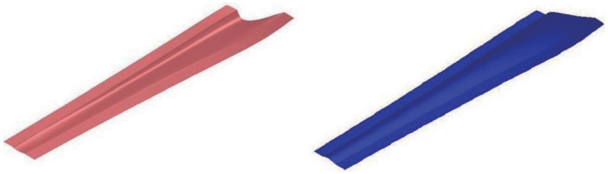

Fig. 12 Mold surfaces for upper (left) and lower (right) parts.

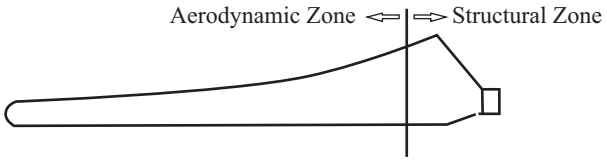

Fig. 13 Aerodynamic and structural zones of a typical wind turbine blade.

5.1 Blade Root Design Considerations

Thus far, we have constructed surfaces that skin airfoil sections. For wind turbine blades, it is also required to connect the circular section of the root to the maximum chord airfoil section. The first proposed procedure treats the circular section as an airfoil section and follows the previously mentioned analyses. But it will introduce undesired curvature variations in the transition region and also the blade's surface is not visually pleasing.

The non-compatibility between the shapes of circle and airfoil is the main source of undesired curvature variations. In order to overcome the problem, we built each half of the blade with two separate skinned surfaces. In other words, two surfaces are considered for structural and aerodynamic zones, see Fig. 13.

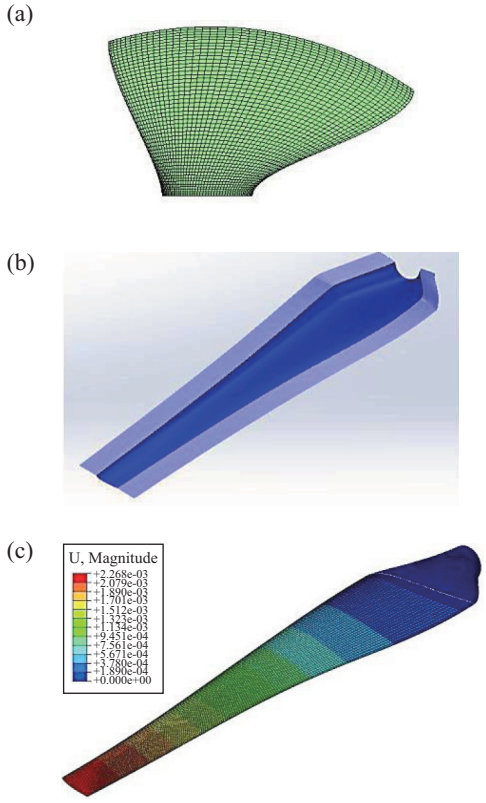

Fig. 14 Examples: (a) A surface for structural zone, (b) upper mold surface and (c) Assembled susrfaces in ABAQUS.

The first surface, which is of structural importance, smoothly connects the circular root section to the first airfoil, while the second surface which is of aerodynamic importance, skins through all airfoil sections. G^1 continuity, this time in v direction, is considered for meeting region of structural and aerodynamic surfaces. Figure 14 represents examples of final surfaces in different software.

6. CONCLUSIONS

The current research suggests dividing the wind turbine blade into two upper and lower parts at early design stage in order to be used directly as the mold surface without any further modifications. The parting line on the leading surface is basically the silhouette curve and G^1 continuity is imposed for upper and lower surfaces. Representing airfoil sections of the blade with two constrained curves lead to less approximation errors and less computational efforts compared to representing by a single curve. The MVS and strain energy fairing criteria show that a two-part surface procedure produces fairer surfaces than a single surface procedure. The proposed algorithms are successfully implemented in a unified MATLAB program. The computed surfaces are then converted into IGES standard file format, which can be easily imported into any CAD and FEM software.

REFRENCES

1. Piegl, L.A. and Tiller, W., *The NURBS Book*, 2nd Edition, Springer, New York, pp. 81-116 (1997).
2. Berry, D. S., *Blade System Design Studies Phase II: Final Project Report*, 1st Edition, Sandia Netional Laboratory, Livermore, pp. 15-45 (2008).
3. Hsu, M. C. *et al*., "An interactive geometry modeling and parametric design platform for isogeometric analysis," *Computers & Mathematics with Applications*, **70**, pp. 1481-1500 (2015).
4. Manwell, J. F., McGowan, J. G. and Rogers, A. L., *Wind energy Explained: Theory Design and Application*, 2nd Edition, John Wiley & Sons, West Sussex, pp. 311-357 (2009).
5. Burton, T., Sharpe, D., Jenkins, N. and Bossanyi, E., *Wind Energy Handbook*, 2nd Edition, John Wiley & Sons, West Sussex, pp. 41-172 (2001).
6. Tangler, J. L. and Somers, D. M., *NREL Airfoil Families for HAWTs*, 1st Edition, National Renewable Energy Laboratory, Golden, pp. 1-12 (1995).
7. Imani, B. M., and Hashemian, S. A., "NURBs-Based Profile Reconstruction using Constrained Fitting Techniques," *Journal of Mechanics*, **28**, pp. 407-412 (2012).
8. Kasik, D. J., Buxton, W. and Ferguson, D. R., "Ten CAD Challenges," *IEEE Computer Graphics and Applications*, **25**, pp. 81-92 (2005).
9. Shamsuddin, S. M., Ahmed, M. A. and Smian, Y., "NURBS skinning surface for ship hull design based on new parameterization method," *International Journal of Advanced Manufacturing Technology*, **28**, pp. 936-941 (2006).
10. Hampsey, M., "Multiobjective Evolutionary Optimisation of Small Wind Turbine Blades," M. S. Thesis, Department of Mechanical Engineering, University of Newcastle, Newcastle, England (2002).
11. Pérez-Arribas, F. and Trejo-Vargas, I., "Computer-aided design of horizontal axis turbine blades," *Renewable Energy*, **44**, pp. 252-260 (2012).
12. Hoschek, J. and Müller, R., "Turbine blade design by lofted B-spline surfaces," *Journal of Computational and Applied Mathematics*, **119**, pp. 235-248 (2000).
13. Pérez, F. and Suárez, J. A., "Quasi-developable B-spline surfaces in ship hull design," *Computer-Aided Design*, **39**, pp. 853-862 (2007).
14. Hyung-Bae, J., "An interpolation method of b-spline surface for hull form design," *International Journal of Naval Architecture and Ocean Engineering*, **2**, pp. 195-199 (2010).
15. Piegl, L. A. and Tiller, W., "Least-Squares B-Spline Curve Approximation with Arbitary End Derivatives," *Eingineering With Computers*, **16**, pp. 109-116 (2000).
16. Park, H., "Lofted B-spline surface interpolation by linearly constrained energy minimization," *Computer-Aided Design*, **35**, pp. 1261-1268 (2003).
17. Piegl, L. A. and Tiller, W., "Reducing control points in surface interpolation," *Computer Graphics and Applications*, **20**, pp. 70-75 (2000).
18. Park, H., Kim, K. and Lee, S. C., "A method for approximate NURBS curve compatibility based on multiple curve refitting," *Computer-Aided Design*, **32**, pp. 237-252 (2000).
19. Moreton, H. P., "Functional optimization for fair surface design," *Proceedings of the 19th annual conference on Computer graphics and interactive techniques,* Chicago, U.S.A. (1992).
20. Soltani, M. R., Birjandi, A. H. and Seddighi Moorani, M., "Effect of surface contamination on the performance of a section of a wind turbine blade," *Scientia Iranica*, **18**, pp. 349-357 (2011).
21. Deshun, L., Rennian, L., Congxin, Y. and Xiuyong, W., "Effects of Surface Roughness on Aerodynamic Performance of a Wind Turbine Airfoil," *Power and Energy Engineering Conference*, Chengdu, China (2010).

(Manuscript received March 14, 2016,
accepted for publication June 20, 2016.)